[177]Lu-lilotomab satetraxetan has the potential to counteract resistance to rituximab in non-Hodgkin's lymphoma

Marion M. Malenge[1,2,3], Sebastian Patzke[1,2], Anne H. Ree[3,4], Trond Stokke[2,] Peter Ceuppens[5], Brian Middleton[5], Jostein Dahle[1] and Ada H. V. Repetto-Llamazares[1].

[1]Nordic Nanovector ASA, Oslo, Norway.

[2]Department of Radiation Biology, Institute for Cancer Research, Oslo University Hospital, Norway

[3]Institute of Clinical Medicine, University of Oslo, Norway

[4]Department of Oncology, Akershus University Hospital, Norway

[5]Inferstats Consulting Ltd, Cheshire, UK

Correspondence:

Jostein Dahle

Kjelsåsveien 168B, 0884 Oslo, Norway

Telephone: +4722183301

jdahle@nordicnanovector.com

First author:

Marion M. Malenge, PhD student

mmalenge@nordicnanovector.com

Running title: ^{177}Lu-lilotomab RIT for NHL

ABSTRACT

Background: Patients with NHL who are treated with rituximab may develop resistant-disease, often associated with changes in expression of CD20. The next generation β-particle emitting radioimmunoconjugate ^{177}Lu-lilotomab-satetraxetan (Betalutin®) was shown to up-regulate CD20 expression in different rituximab-sensitive NHL cell lines and to act synergistically with rituximab in a rituximab-sensitive NHL animal model. We hypothesized that ^{177}Lu-lilotomab-satetraxetan may be used to reverse rituximab-resistance in NHL.

Methods: The rituximab-resistant Raji2R and the parental Raji cell lines were used. CD20 expression was measured by flow cytometry. ADCC was measured by a bioluminescence reporter assay. The efficacies of combined treatments with ^{177}Lu-lilotomab-satetraxetan (150MBq/kg or 350MBq/kg) and rituximab (4×10mg/kg) were compared with those of single agents or saline in a Raji2R-xenograft model. Cox-regression and the Bliss independence model were used to assess synergism.

Results: Rituximab-binding in Raji2R cells was 36±5% of that in the rituximab-sensitive Raji cells. ^{177}Lu-lilotomab-satetraxetan treatment of Raji2R cells increased the binding to 53±3% of the parental cell line. Rituximab ADCC-induction in Raji2R cells was 20±2% of that induced in Raji cells, while treatment with ^{177}Lu-lilotomab-satetraxetan increased the ADCC-induction to 30±3% of Raji cells, representing a 50% increase ($p<0.05$). The combination of rituximab with 350MBq/kg ^{177}Lu-lilotomab-satetraxetan synergistically suppressed Raji2R tumor growth in athymic $Foxn1^{nu}$ mice.

Conclusion: ^{177}Lu-lilotomab-satetraxetan has the potential to reverse rituximab-resistance; it can increase rituximab-binding and ADCC-activity *in-vitro* and can synergistically improve anti-tumor efficacy *in-vivo*.

INTRODUCTION

Non-Hodgkin's lymphoma (NHL) is the most common hematological malignancy and had the eleventh highest mortality-rate of all malignancies worldwide in 2018(*1,2*). B-lymphocytes are predominantly the origin of NHL, with malignant B-cells expressing a high density of specific antigens such as CD20 and CD37 on their surface(*3*). These antigens provide a platform for antibody-based targeted therapies(*4*). Immunotherapy with the CD20-directed antibody rituximab inhibits cell proliferation by inducing antibody-dependent cellular cytotoxicity (ADCC) and complement-dependent cytotoxicity (*5*). Although rituximab alone and in combination with chemotherapy are a mainstay of NHL treatment(*6-8*), the efficacy is variable(*9*). Some patients are reported to have disease progression after initial response to rituximab(*10*). Conversely, rituximab-naïve patients have been reported with primarily rituximab-refractory disease(*11*).

The mechanisms of rituximab-resistance are not completely understood(*9,12*). Rituximab-resistance is postulated to be a result of down-regulation of the CD20 gene, internalization, lysosomal degradation and shaving off of rituximab/CD20 complexes(*13-18*). Strategies to counteract rituximab-resistance include combination therapies and targeting of alternative antigens. Previous studies have described the ability of ionizing radiation to potentiate immunotherapy through the generation of reactive-oxygen species that mediates an increase in antigen expression(*19-21*), consequently improving on antibody-dependent toxicity in addition to the direct cytotoxic radiation effect(*21,22*). Anti-CD20 antibody binding increased up to two-fold, 20-120 hours after irradiation(*19,20,23*). Radioimmunotherapy delivers targeted short-range radiation that effectively ablates malignant cells and with limited toxicity to normal tissues(*24,25*).

The anti-CD37 radioimmunoconjugate ^{177}Lu-lilotomab-satetraxetan (^{177}Lu-lilotomab), consisting of the β-emitting isotope lutetium-177 ($T_{1/2} = 6.7$days) chelated to a chemical linker p-SCN-benzyl-DOTA (satetraxetan) conjugated to the murine antibody lilotomab, has shown robust anti-tumor activity and low toxicity in preclinical models[26,27]. ^{177}Lu-lilotomab is currently in clinical trials for relapsed/ refractory lymphomas (NCT01796171, NCT02658968)[25,28].

We have recently shown that pre-treatment of rituximab-sensitive NHL cells with ^{177}Lu-lilotomab increases CD20 binding *in-vitro* and synergistically increases the anti-tumor effect when combined with rituximab *in-vivo*[23]. Currently, ^{177}Lu-lilotomab is tested in combination with rituximab in patients with previously treated follicular lymphoma(NCT03806179).

Here, we hypothesized that ^{177}Lu-lilotomab can reverse rituximab-resistance in NHL. We employed a rituximab-resistant NHL cell line and animal model and explored the mechanism of synergy by measuring rituximab-binding and ADCC-induction and apoptosis.

MATERIALS AND METHODS

Cell Lines

Burkitt lymphoma cell lines Raji and Raji2R, from Roswell Park Institute[16], were cultured in RPMI medium (Thermofisher, USA) supplemented with Glutamax, 10% heat inactivated fetal bovine serum and 1% penicillin-streptomycin at 37°C with 5% CO_2.

Radiolabeling of Antibodies with ^{177}Lu

Lilotomab-satetraxetan was pH-adjusted using ammonium acetate then radiolabeled with ^{177}Lu (ITG, Germany) at 37°C for 15–30 minutes. The specific activity for all *in-vitro* studies was 600MBq/mg, while 200MBq/mg was chosen for *in-vivo* studies. The radiochemical purity and

immunoreactive fraction of the conjugate were determined using instant thin layer chromatography and by a modified Lindmo method*(29)* respectively.

Measurement of CD20 Binding

Cells at a concentration of 2.5×10^6 cells/ml were incubated for 18 hours with 0-20µg/ml of either lilotomab, ^{177}Lu-lilotomab or saline (PBS, control) at 37°C. The cells were then washed, resuspended in fresh medium to a concentration of 0.5×10^6 cells/ml and cultured up to 6 days, with fresh medium added on day 3. On days 3 and 6, the cells were prepared for flow cytometric assays using rituximab (Roche, Switzerland) conjugated to Alexa-Fluor647 tetra fluorophenyl ester (Thermofisher) according to the manufacturer's instructions. The cell concentration was adjusted to 1×10^6 cells/ml and Raji cells stained with 0.4µg/ml Hoechst 33342 (Life technologies, USA) for identity barcoding, at 37°C for 20 minutes then washed using ice-cold PBS. To assess the effect of ^{177}Lu-lilotomab treatment on CD20 binding, the cells were incubated at 4°C with 30µg/ml rituximab-Alexa647 for 30 minutes. To estimate the background signal, cells were incubated with 100-fold excess of non-fluorescent rituximab before addition of rituximab-Alexa647.

Cells were washed and fluorescence was read by flow cytometry (Guava® easyCyte12HT, Millipore). Changes in rituximab-binding on ^{177}Lu-lilotomab treated cells relative to control cells for each cell line were assessed using equation 1.

$$Increase\ in\ rituximab\ binding = \frac{Rituximab\ binding\ (treated - control)cells}{Rituximab\ binding\ (control)cells} \times 100$$

(1)

Rituximab-binding in rituximab-resistant Raji2R cells (control and treated cells) was compared to rituximab-binding in untreated (control) rituximab-sensitive Raji cells using equation 2.

$$Relative\ rituximab\ binding = \frac{Rituximab\ binding\ of\ \ Raji2R}{Rituximab\ binding\ of\ Raji\ (control)} \times 100$$

<div align="right">(2)</div>

Measurement of ADCC

The cells at a concentration of 2.5×10^6 cells/ml were incubated with 1µg/ml of either lilotomab, ^{177}Lu-lilotomab or controls at 37°C for 18 hours. All cells were washed and adjusted to 0.5×10^6 cells/ml in fresh medium before further incubated . After 6 days, rituximab-induced ADCC-activity was measured using ADCC reporter bioassay kits (Promega, USA) containing Jurkat cells engineered to stably express FcγRIIIa receptor(*30*) as effector cells. These cells have a firefly luciferase gene driven by a nuclear factor of activated T-cells response element reporting the activation of the gene by producing luciferase quantified as luminescence signal. The cells were co-incubated with 0.68-40µg/ml rituximab and effector cells for 22 hours at a 2:1 effector:target cells ratio. ADCC-activity was measured as the luminescence of cell-bound effector cells. Change in ADCC-induction by rituximab in ^{177}Lu-lilotomab treated cells relative to control cells was obtained using equation 3.

$$Increase\ in\ \ ADCC\ induction = \frac{ADCC\ induction\ in\ cells\ (treated - control)}{ADCC\ induction\ in\ cells\ (control)} \times 100$$

<div align="right">(3)</div>

Relative ADCC-induction by rituximab in Raji2R control and ^{177}Lu-lilotomab treated cells to Raji control cells was obtained using equation 4.

$$Relative\ \ ADCC\ induction = \frac{ADCC\ induction\ in\ Raji2R}{ADCC\ induction\ in\ Raji\ (control)} \times 100$$

<div align="right">(4)</div>

In-vivo Xenograft Model

All procedures in this study were approved by The Norwegian Animal Research Authority (NARA) and performed in accordance to NARA regulations and Federation of European Laboratory Animal Science Associations (FELASA) recommendations. Female athymic nude $Foxn1^{nu}$ mice bred at the Institute for Comparative Medicine, Oslo University Hospital, Norway were used.

The mice, aged 4-5 weeks old with an average weight of 21±2g, were injected subcutaneously in both flanks with $10×10^6$ Raji2Rcells/flank using a 1:1 Matrigel dilution ratio. Mice were injected intraperitoneally with 50µl of anti-asialo GM1 (Wako Chemicals, USA) after dilution per manufacturers recommendation, 24 hours prior to cell inoculation and once every week thereafter for the rest of the study. This was administered to increase tumor-take and prevent spontaneous tumor regressions by decreasing the natural killer (NK) cell population in the mice. On attaining tumor diameter between 4mm and 11mm, the mice were placed into treatment groups of 10 mice each, ensuring similar average tumor volumes per group.

Therapy Study

Raji2R-xenografted mice were administered with *i)*NaCl, *ii)*rituximab monotherapy administered as 4 subsequent doses every 3-4 days (4×10mg/kg), *iii)*150MBq/kg of ^{177}Lu-lilotomab as monotherapy, *iv)*350MBq/kg of ^{177}Lu-lilotomab as monotherapy, *v)*combination therapy of 150MBq/kg ^{177}Lu-lilotomab and rituximab (4×10mg/kg) and *vi)*combination therapy of 350MBq/kg ^{177}Lu-lilotomab and rituximab (4×10mg/kg). The dosing concentrations of ^{177}Lu-lilotomab were below the maximum tolerated dose (around 550MBq/kg) in nude mice[27]. The 2 chosen dosing concentrations were considered to be therapeutically suboptimal without the

combination with rituximab, which would make it feasible to observe any synergistic effect of the combination.

Caliper measurements of the tumors in 3-dimensions were recorded 2-3 times a week. Tumor volume was calculated as $\frac{\pi}{6}(Length \times Width \times Height)$. Animal health status was monitored for the length of the study and animals were euthanized by cervical dislocation when tumor diameter was >20mm or animals were observed to experience severe poor health, tumor-necrosis or ulceration, weight gain or loss >10% from maximum or minimum recorded weight or any other signs of discomfort. During euthanasia, the animal was dissected to observe for any anatomical anomalies.

Statistical Analysis

In-vitro data was analyzed in SigmaPlot 13.0 (Systat, USA) and Prism 8 (GraphPad, USA) using two-tailed t-tests on either complete data sets or paired averaged data, to compare the different groups, cell lines and timepoints. Data is presented as mean±standard error (SE) and p<0.05 was considered statistically significant.

Mouse survival was defined as time to the event of death due to tumor diameter >20mm (representative of disease progression). The analysis was performed in SigmaPlot using the Log-rank test reporting statistical significance by Holm-Sidak test for multiple comparisons.

Tumor volume was computed in two different ways: as average±SE for each group, maintaining tumor volume constant after euthanasia along the 70 days of the study and by extrapolation of tumor volume after euthanasia which is considered a better representation of the data but can only be performed up to 20 days due to tumor volumes becoming infeasibly large. SAS 9.4 (SAS, USA) was used for these calculations.

Bliss independence model was used to evaluate synergy in the *in-vivo* study using the extrapolated tumor volumes. Difference from baseline was calculated on the log-scale and all statistical analysis were performed on the log-transformed data.

Bliss analysis of mice survival was performed by fitting a Cox Proportional-Hazard model to the survival data. The Bliss definition of synergy was assessed by the interaction of the combination treated groups with the rituximab and respective ^{177}Lu-lilotomab monotherapy groups. Interaction values lower than 1 were considered synergistic and statistical significance defined both by $p<0.05$ and an interaction value $\pm90\%$ confidence interval <1. R (2019) with survival package was used for these calculations.

RESULTS

Increased Rituximab-Binding by ^{177}Lu-lilotomab

Exposure of Raji and Raji2R cells to ^{177}Lu-lilotomab resulted in a dose-dependent increase in rituximab-binding as compared with control cells (Fig. 1). Increase in rituximab-binding (equation 1) was fitted using a regression line based on the two-parameter exponential rise to maximum equation (R^2 values between 0.71 and 0.90). Rituximab-binding in ^{177}Lu-lilotomab treated Raji cells continuously increased when compared to the control, reaching 78% 3 days after treatment (Fig. 1A). Six days after treatment, rituximab-binding showed an initial exponential increase from the control, followed by a plateau at 31% for ^{177}Lu-lilotomab concentrations above 0.5μg/ml. The same was observed in Raji2R cells with a plateau at 25% for 3 days and at 68% for 6 days after ^{177}Lu-lilotomab treatment (Fig.1B). The increase in rituximab-binding at 3 days was significantly different from that at 6 days in both cell lines ($p<0.01$).

Binding in Raji cells was highest at 3 days after treatment while in Raji2R cells it was highest at 6 days.

In order to compare the relative rituximab-binding of Raji2R versus Raji cells (equation 2), the maximum asymptote of the fitted curves in Fig. 1B were used. Rituximab-binding in Raji2R cells was on average 36±5% of the binding in Raji cells when no ^{177}Lu-lilotomab was given (equation 2, Fig. 1C).

After treatment with ^{177}Lu-lilotomab the relative binding to Raji2R cells compared to untreated Raji cells increased to 47±1% (p<0.01) at 3 days and 53±3% (p<0.01) at 6 days. In contrast, treatment with unlabelled lilotomab or PBS had no effect on rituximab-binding (data not shown).

Enhanced ADCC by Rituximab after ^{177}Lu-lilotomab Treatment

ADCC-induction was assessed by measurement of effector-cell binding of cell-bound rituximab in cells previously treated with ^{177}Lu-lilotomab or PBS (control). There was no significant change in effector-cell binding of rituximab in Raji cells after treatment with ^{177}Lu-lilotomab (Fig. 2A, p>0.05). Conversely, treatment of Raji2R cells with ^{177}Lu-lilotomab significantly augmented effector-cell binding (p<0.05, Fig. 2B). The maximum asymptote of the fitted curves from Figs. 2A and B were used to calculate the increase in ADCC-induction and the relative increase in ADCC-induction in Raji2R vs Raji cells (equations 3 and 4 respectively). Effector-cell binding increased by 47±4% in ^{177}Lu-lilotomab treated Raji2R cells compared with untreated Raji2R cells (equation 3). Effector-cell binding in ^{177}Lu-lilotomab treated Raji2R cells was 43% higher than in untreated Raji2R cells relative to untreated Raji cells (30±3% versus 21±2%, equation 4, p<0.05, Fig. 2C). Unlabelled lilotomab did not modulate effector-cell binding (data not shown).

Synergistic Anti-tumor Efficacy of the Combination of ^{177}Lu-lilotomab and Rituximab

Treatment of Raji2R-xenografted mice with rituximab alone did not suppress tumor growth compared to that in mice treated with saline (Fig. 3). However, treatment with ^{177}Lu-lilotomab alone or in combination with rituximab showed inhibition of tumor growth when compared to the saline and rituximab-treated tumors. This inhibition was reflected in the lower fold change in tumor volume from baseline at various time points after start of treatment with the combination of 150MBq/kg or 350MBq/kg ^{177}Lu-lilotomab and rituximab compared with monotherapy of the respective treatments ($p<0.05$, Table 1). The Bliss independence model indicated significant synergism in combining 350MBq/kg ^{177}Lu-lilotomab with rituximab ($p<0.05$ for tumor volumes measured 17 and 20 days after treatment), while the combination of 150MBq/kg ^{177}Lu-lilotomab and rituximab did not reach statistical significance for any time point (Fig. 3A). When analyzing the tumor volume data in the duration of the study (by maintaining last tumor volume after euthanasia) a significant difference was found between the 350MBq/kg ^{177}Lu-lilotomab monotherapy and the respective combination with rituximab (Fig. 3B, $p<0.05$), indicating that ^{177}Lu-lilotomab potentiated the rituximab-effect.

Treatment with ^{177}Lu-lilotomab alone and in combination with rituximab significantly prolonged time-to-event compared to saline and rituximab-treatment (Fig. 4, Table 2). The median survival time of mice treated with the combination of 350MBq/kg ^{177}Lu-lilotomab and rituximab was doubled when compared to survival of mice given 350MBq/kg ^{177}Lu-lilotomab monotherapy and it was 5 times longer than for mice given rituximab monotherapy.

Bliss independence analysis did not provide statistically significant results (Table 3). The lack of significance might be due to the large number of censored animals and the poor Proportional-Hazards assumption in the Cox model ($p=0.048$).

A total of 14 mice out of 60 included in the study were euthanized due to tumor-ulceration (Fig. 5). Most of the ulcers appeared in mice given ^{177}Lu-lilotomab monotherapy or the combination with rituximab. These mice were regarded as censored in the survival analysis since the tumors did not reach the primary end point (tumor diameter >20mm).

An alternative time-to-event analysis using tumor diameter >20mm or tumor-ulceration as end point was performed (Supplemental Fig. 1). Median survival times were slightly different (Supplemental Table 1) but the outcome of Bliss independence analysis did not provide statistically significant results (Supplemental Table 2).

DISCUSSION

Although immunotherapy with rituximab has been widely successful, rituximab-resistance in subsets of NHL patients remains a challenge in clinical management of the disease. In the present study, we demonstrated that *in-vitro* treatment of rituximab-resistant Raji2R cells with ^{177}Lu-lilotomab increased both rituximab-binding and ADCC-activity. In addition, we showed that *in-vivo* combination of ^{177}Lu-lilotomab with rituximab can synergistically suppress tumor growth in Raji2R-xenografted mice.

Evidence supports that ADCC-activity may be the predominant *in-vivo* mechanism of action of rituximab[31,32]. We have therefore explored if ^{177}Lu-lilotomab can restore ADCC by rituximab in the rituximab-resistant Raji2R cellline. Our findings show that partial restoration can be reached. The increased ADCC may be caused by the significant time-dependent increase in rituximab-binding, an observation in line with results presented by Hiraga et al.[13], who hypothesized the delay to be due to altered transcriptional regulation resulting from persistent rituximab-treatment during acquisition of resistance. In agreement with observations by van Meerten et al.[33] the direct cytotoxic or apoptotic effect of rituximab in the rituximab-sensitive

Raji cells was negligible (Supplemental Fig. 2 and 3) and therefore it was not possible to study the sensitization of rituximab-resistant cells to rituximab by ^{177}Lu-lilotomab using this model. Further studies using other rituximab-resistant cell lines are warranted.

Translation of the *in-vitro* results to a clinical setting is limited. The dose delivered from ^{177}Lu-lilotomab to cells in the *in-vitro* studies is a function of both specific and non-specific irradiation of the cells during the 18hours incubation time(*34*). Given that CD20 upregulation is mediated by intracellular redox regulation and is dose-dependent(*19,23*), we expect that treatment with a non-specific radioimmunoconjugate will produce a similar increase in CD20 binding and subsequent ADCC increase in this experimental set-up. However, in an *in-vivo* or clinical setting, ^{177}Lu-lilotomab would have an important advantage over a non-specific radioimmunoconjugate due to its capability to deliver targeted radiation to tumor while sparing the healthy tissues.

Although the time-to-event for mice treated with the combination of ^{177}Lu-lilotomab and rituximab was not significantly synergistic, there was significant synergy in tumor growth delay. We have shown that *in-vivo* combination therapy with ^{177}Lu-lilotomab and rituximab has the potential to synergistically suppress tumor growth in Raji2R-xenografted mice. The increased rituximab-binding and enhanced ADCC shown in our *in-vitro* studies are among the mechanisms of action that that could lead to the observed synergy.

Other mechanisms that might contribute to the observed synergy are improved complement-dependent cytotoxicity by colocalization of CD37 and CD20 on the cell membrane(*35*), radiation-induced permeability of tumor vasculature(*36*), radiation-induced immunogenic modulation of tumor cells(*37-39*), rituximab-induced sensitization of tumor cells to ionizing radiation(*40*) and rituximab-induced increased internalization of CD37*(41)* leading to increased cellular retention of ^{177}Lu and thus to a higher cellular absorbed radiation dose(*25*).

In order to have good tumor-take and growth, our animal model required use of anti-asialo antibody to decrease the amount of NK cells, which are the classical mediators of ADCC. This intentional decrease in NK cell numbers might have led to a reduced ADCC effect. The observed ADCC effect in our animal studies was probably exerted by the remaining NK cells and other effector cells such as neutrophils and monocytes. The observed tumor-ulceration seemed to be related to treatment efficacy. Only one ulcer was observed in the control mice and no ulcers were observed in the rituximab-treated mice while the number of ulcers increased with increasing dose of ^{177}Lu-lilotomab. Ulceration could therefore be due to the accelerated tumor necrosis caused by the therapy. The probable cause of the observed ulceration is the proximity of the s.c tumor xenografts to the mouse skin.

We have shown in previous studies that ^{177}Lu-lilotomab can synergize with rituximab in rituximab-sensitive cell lines. In the current study we have taken the analysis one step further and shown that synergy can also be observed in rituximab-resistant cell lines and that rituximab-resistance might be partially reversed by combining rituximab with ^{177}Lu-lilotomab. Further studies using different rituximab-resistant cell lines and animal models with an intact immune system might be of interest in order to generalize our findings and gain deeper insight into the mechanisms of action behind the observed synergy.

The current results further support the rationale underlying the current clinical phase 1b trial (Archer-1; NCT03806179) of combination treatment of patients with relapsed/refractory follicular lymphoma and suggest that in the future ^{177}Lu-lilotomab radioimmunotherapy could potentially be used for re-sensitization of relapsed/ refractory NHL patients to CD20 targeting therapy.

CONCLUSION

In this present work, we have demonstrated that radioimmunotherapy with ^{177}Lu-lilotomab has the potential to reverse rituximab-resistance through increased rituximab-binding and ADCC-activity in rituximab-resistant NHL models.

DISCLOSURE

KEYPOINTS

QUESTION: Can ^{177}Lu-lilotomab reverse rituximab-resistance and improve efficacy of rituximab-therapy?

PERTINENT FINDINGS: ^{177}Lu-lilotomab significantly increases rituximab-binding and rituximab-mediated ADCC-activity and when in combination with rituximab, has the potential to synergistically suppressed tumor growth in an NHL mouse model.

IMPLICATIONS FOR PATIENT CARE: ^{177}Lu-lilotomab could potentially be used for re-sensitization of relapsed/ refractory NHL patients to CD20 targeting therapy.

REFERENCES

1.   Siegel RL, Miller KD, Jemal A. Cancer Statistics, 2017. *CA Cancer J Clin.* 2017;67:7-30.

2.   Bray F, Ferlay J, Soerjomataram I, Siegel RL, Torre LA, Jemal A. Global cancer statistics 2018: GLOBOCAN estimates of incidence and mortality worldwide for 36 cancers in 185 countries. *CA Cancer J Clin.* 2018;68:394-424.

3.   Malcolm TI, Hodson DJ, Macintyre EA, Turner SD. Challenging perspectives on the cellular origins of lymphoma. *Open Biol.* 2016;6:1-12.

4.   Del Bufalo F, Merli P, Alessi I, Locatelli F. B-cell depleting immunotherapies: therapeutic opportunities and toxicities. *Expert Rev Clin Immunol.* 2019;15:497-509.

5.   Reff ME, Carner K, Chambers KS, et al. Depletion of B cells in vivo by a chimeric mouse human monoclonal antibody to CD20. *Blood.* 1994;83:435-445.

6.   Mounier N, Briere J, Gisselbrecht C, et al. Rituximab plus CHOP (R-CHOP) overcomes bcl-2--associated resistance to chemotherapy in elderly patients with diffuse large B-cell lymphoma (DLBCL). *Blood.* 2003;101:4279-4284.

7.   Petryk M, Grossbard ML. Rituximab therapy of B-cell neoplasms. *Clin Lymphoma.* 2000;1:186-194.

8.   Davis TA, Grillo-Lopez AJ, White CA, et al. Rituximab anti-CD20 monoclonal antibody therapy in non-Hodgkin's lymphoma: safety and efficacy of re-treatment. *J Clin Oncol.* 2000;18:3135-3143.

9.   Rezvani AR, Maloney DG. Rituximab resistance. *Best Pract Res Clin Haematol.* 2011;24:203-216.

10.   Davis TA, Czerwinski DK, Levy R. Therapy of B-cell lymphoma with anti-CD20 antibodies can result in the loss of CD20 antigen expression. *Clin Cancer Res.* 1999;5:611-615.

11.   Colombat P, Salles G, Brousse N, et al. Rituximab (anti-CD20 monoclonal antibody) as single first-line therapy for patients with follicular lymphoma with a low tumor burden: clinical and molecular evaluation. *Blood.* 2001;97:101-106.

12.   Duman BB, Sahin B, Ergin M, Guvenc B. Loss of CD20 antigen expression after rituximab therapy of CD20 positive B cell lymphoma (diffuse large B cell extranodal marginal zone lymphoma combination): a case report and review of the literature. *Med Oncol.* 2012;29:1223-1226.

13.   Hiraga J, Tomita A, Sugimoto T, et al. Down-regulation of CD20 expression in B-cell lymphoma cells after treatment with rituximab-containing combination chemotherapies: its prevalence and clinical significance. *Blood.* 2009;113:4885-4893.

14.   Miyoshi H, Arakawa F, Sato K, et al. Comparison of CD20 expression in B-cell lymphoma between newly diagnosed, untreated cases and those after rituximab treatment. *Cancer Sci.* 2012;103:1567-1573.

15.   Tokunaga T, Tomita A, Sugimoto K, et al. De novo diffuse large B-cell lymphoma with a CD20 immunohistochemistry-positive and flow cytometry-negative phenotype: molecular mechanisms and correlation with rituximab sensitivity. *Cancer Sci.* 2014;105:35-43.

16.   Czuczman MS, Olejniczak S, Gowda A, et al. Acquirement of rituximab resistance in lymphoma cell lines is associated with both global CD20 gene and protein down-regulation regulated at the pretranscriptional and posttranscriptional levels. *Clin Cancer Res.* 2008;14:1561-1570.

17.   Beers SA, French RR, Chan HT, et al. Antigenic modulation limits the efficacy of anti-CD20 antibodies: implications for antibody selection. *Blood.* 2010;115:5191-5201.

18.   Beum PV, Kennedy AD, Williams ME, Lindorfer MA, Taylor RP. The shaving reaction: rituximab/CD20 complexes are removed from mantle cell lymphoma and chronic lymphocytic leukemia cells by THP-1 monocytes. *J Immunol.* 2006;176:2600-2609.

19.   Gupta D, Crosby ME, Almasan A, Macklis RM. Regulation of CD20 expression by radiation-induced changes in intracellular redox status. *Free Radic Biol Med.* 2008;44:614-623.

20.   Kunala S, Macklis RM. Ionizing radiation induces CD20 surface expression on human B cells. *Int J Cancer.* 2001;96:178-181.

21.   Wattenberg MM, Kwilas AR, Gameiro SR, Dicker AP, Hodge JW. Expanding the use of monoclonal antibody therapy of cancer by using ionising radiation to upregulate antibody targets. *Br J Cancer.* 2014;110:1472-1480.

22.   Weber T, Botticher B, Mier W, et al. High treatment efficacy by dual targeting of Burkitt's lymphoma xenografted mice with a (177)Lu-based CD22-specific radioimmunoconjugate and rituximab. *Eur J Nucl Med Mol Imaging.* 2016;43:489-498.

23.   Repetto-Llamazares AHV, Malenge MM, O'Shea A, et al. Combination of (177) Lu-lilotomab with rituximab significantly improves the therapeutic outcome in preclinical models of non-Hodgkin's lymphoma. *Eur J Haematol.* 2018;101:522-531.

24.   Multani P. Development of radioimmunotherapy for the treatment of non-Hodgkin's lymphoma. *Int J Hematol.* 2002;76:401-410.

25.   Dahle J, Repetto-Llamazares AH, Mollatt CS, et al. Evaluating antigen targeting and anti-tumor activity of a new anti-CD37 radioimmunoconjugate against non-Hodgkin's lymphoma. *Anticancer Res.* 2013;33:85-95.

26.   Repetto-Llamazares AH, Larsen RH, Patzke S, et al. Targeted cancer therapy with a novel anti-CD37 beta-particle emitting radioimmunoconjugate for treatment of non-Hodgkin lymphoma. *PLoS One.* 2015;10:e0128816.
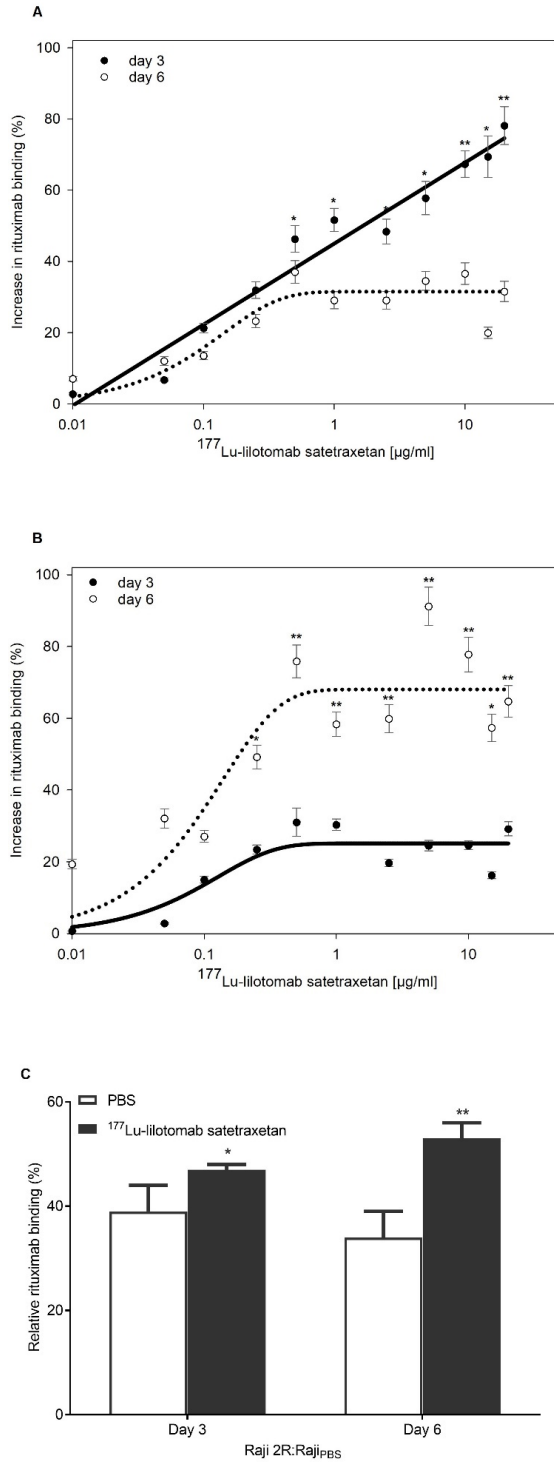
27.   Repetto-Llamazares AH, Larsen RH, Giusti AM, et al. 177Lu-DOTA-HH1, a novel anti-CD37 radio-immunoconjugate: a study of toxicity in nude mice. *PLoS One.* 2014;9:e103070.

28.   Kolstad A, Madsbu U, Beasley M, et al. Lymrit 37-01: Updated results of a phase I/II study of 177Lu-lilotomab satetraxetan, a novel CD37-targeted antibody-radionuclide-conjugate in relapsed NHL patients. *Hematol Oncol.* 2017;35:269-270.
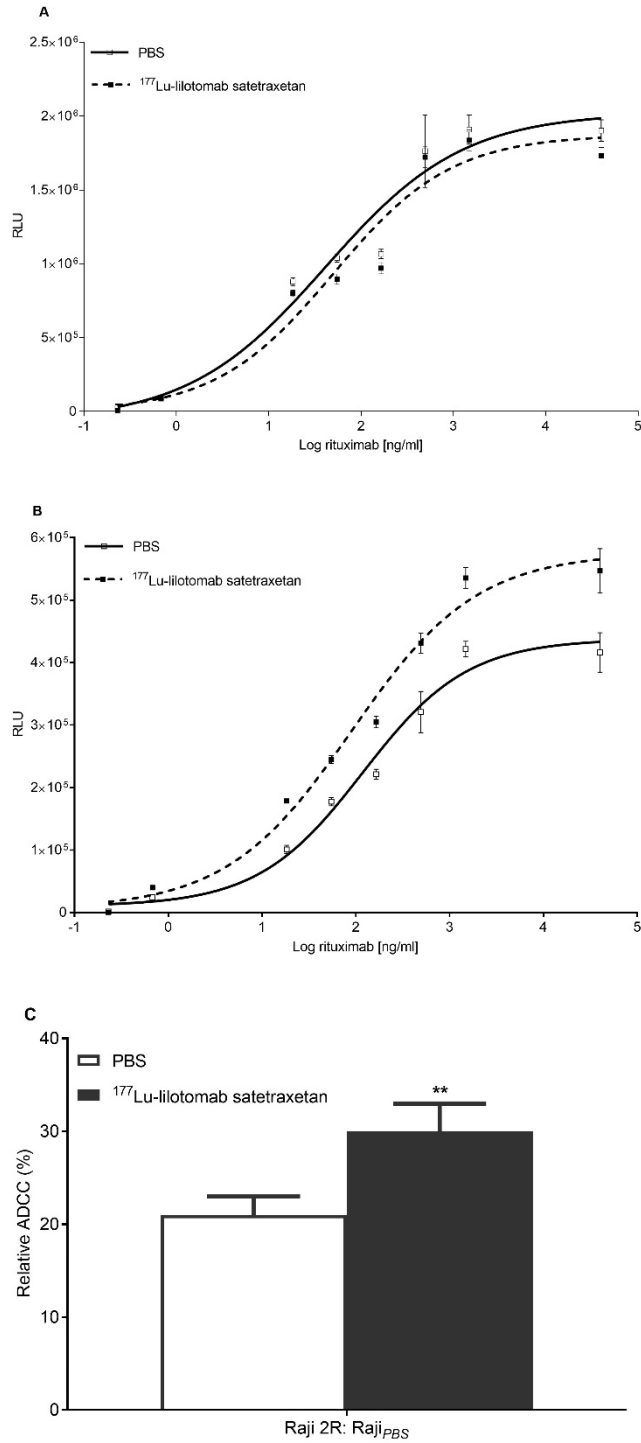
29.   Lindmo T, Boven E, Cuttitta F, Fedorko J, Bunn PA, Jr. Determination of the immunoreactive fraction of radiolabeled monoclonal antibodies by linear extrapolation to binding at infinite antigen excess. *J Immunol Methods.* 1984;72:77-89.

30.   Parekh BS, Berger E, Sibley S, et al. Development and validation of an antibody-dependent cell-mediated cytotoxicity-reporter gene assay. *MAbs.* 2012;4:310-318.

31.   Clynes RA, Towers TL, Presta LG, Ravetch JV. Inhibitory Fc receptors modulate in vivo cytotoxicity against tumor targets. *Nat Med.* 2000;6:443-446.

32.   Hernandez-Ilizaliturri FJ, Jupudy V, Ostberg J, et al. Neutrophils contribute to the biological antitumor activity of rituximab in a non-Hodgkin's lymphoma severe combined immunodeficiency mouse model. *Clin Cancer Res.* 2003;9:5866-5873.

33.   van Meerten T, van Rijn RS, Hol S, Hagenbeek A, Ebeling SB. Complement-induced cell death by rituximab depends on CD20 expression level and acts complementary to antibody-dependent cellular cytotoxicity. *Clin Cancer Res.* 2006;12:4027-4035.

34.   Marcatili S, Pichard A, Courteau A, et al. Realistic multi-cellular dosimetry for 177Lu-labelled antibodies: model and application. *Phys Med Biol.* 2016;61:6935-6952.

35.   Oostindie SC, van der Horst HJ, Lindorfer MA, et al. CD20 and CD37 antibodies synergize to activate complement by Fc-mediated clustering. *Haematologica.* 2019;104:1841-1852.

36.   Heyerdahl H, Abbas N, Sponheim K, Mollatt C, Bruland O, Dahle J. Targeted alpha therapy with 227Th-trastuzumab of intraperitoneal ovarian cancer in nude mice. *Curr Radiopharm.* 2013;6:106-116.

37.   Chakraborty M, Abrams SI, Camphausen K, et al. Irradiation of tumor cells up-regulates Fas and enhances CTL lytic activity and CTL adoptive immunotherapy. *J Immunol.* 2003;170:6338-6347.

38.   Chakraborty M, Abrams SI, Coleman CN, Camphausen K, Schlom J, Hodge JW. External beam radiation of tumors alters phenotype of tumor cells to render them susceptible to vaccine-mediated T-cell killing. *Cancer Res.* 2004;64:4328-4337.

39.   Reits EA, Hodge JW, Herberts CA, et al. Radiation modulates the peptide repertoire, enhances MHC class I expression, and induces successful antitumor immunotherapy. *J Exp Med.* 2006;203:1259-1271.

40.   Kapadia NS, Engles JM, Wahl RL. In vitro evaluation of radioprotective and radiosensitizing effects of rituximab. *J Nucl Med.* 2008;49:674-678.

41.   Hicks SW, Lai KC, Gavrilescu LC, et al. The antitumor activity of IMGN529, a CD37-targeting antibody-drug conjugate, is potentiated by rituximab in non-Hodgkin lymphoma Models. *Neoplasia.* 2017;19:661-671.

Fig. 1 Increase in rituximab-binding on days 3 (solid lines) and 6 (dotted lines) after treatment with escalating doses of ^{177}Lu-lilotomab in (A) Raji cells and (B) Raji2R cells. (C) Rituximab-binding in Raji2R cells relative to untreated Raji cells when considering the average of the horizontal plateau from Fig. B. *p<0.05 and **p<0.005, N=3.

Fig. 2 Luminescence (RLU) representative of effector-cell binding to rituximab in (A) Raji and (B) Raji2R cells treated with 1μg/ml ^{177}Lu-lilotomab or PBS (untreated). (C) Relative change in effector-cell binding to rituximab in untreated and in 1μg/ml ^{177}Lu-lilotomab treated Raji2R cells relative to untreated Raji cells, **p<0.05, N=3-4.
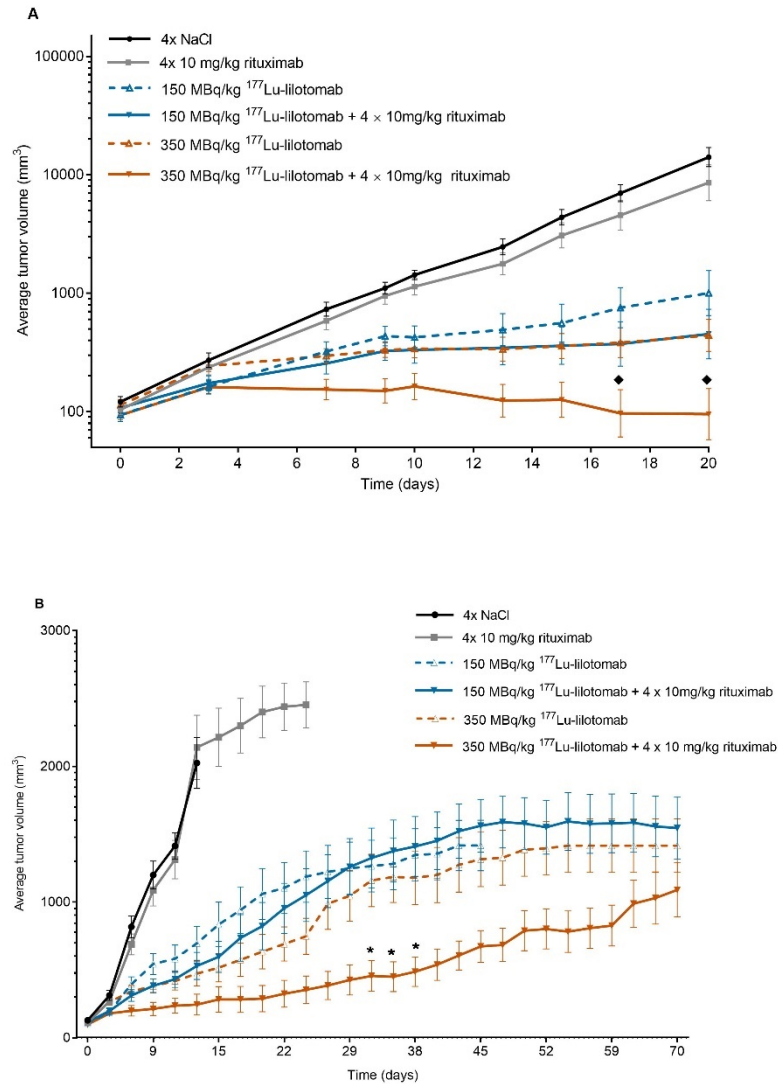
*Fig. 3 Average tumor volume±SE in Raji2R-xenografted mice treated with saline, rituximab, 150MBq/kg and 350MBq/kg ^{177}Lu-lilotomab monotherapy or combination with rituximab. N=10. (A) Curve built using extrapolation of tumor volumes after euthanasia, ♦ timepoints of observed significant synergistic effects (p<0.05) (B) Curve built keeping constant tumor volume after euthanasia, *timepoints observed to be significantly different from ^{177}Lu-lilotomab monotherapy*
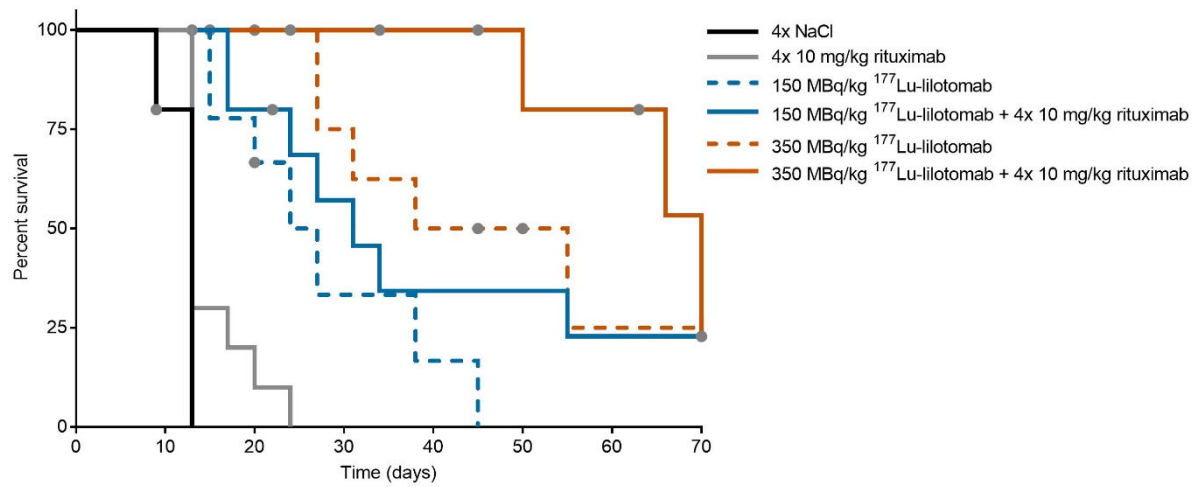
(p<0.05).

Fig. 4 Kaplan-Meier survival curves of Raji2R-xenografted mice treated with saline, rituximab, 150MBq/kg and 350MBq/kg ^{177}Lu-lilotomab monotherapy or combination with rituximab. N=10. End point: tumor diameter larger than 20mm. Gray dots: censored animals.
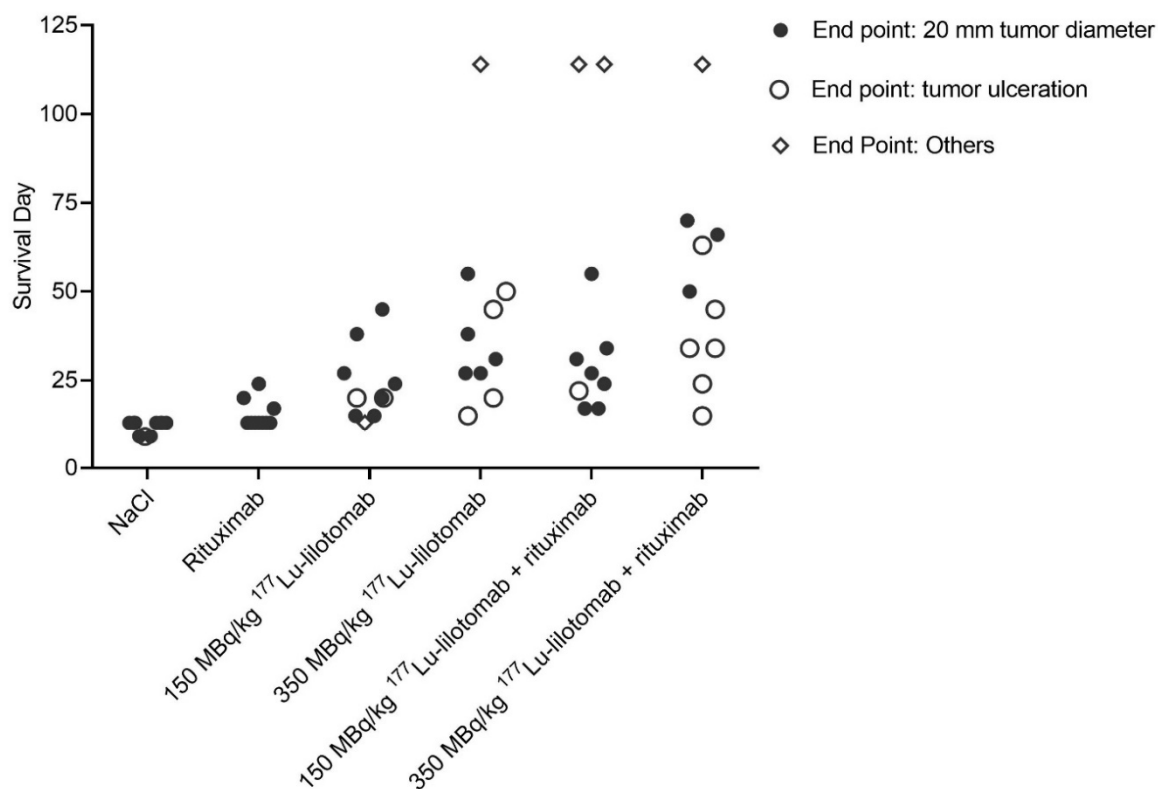
Fig. 5 Survival of Raji2R-xenografted mice treated with saline, rituximab, 150MBq/kg and 350MBq/kg ^{177}Lu-lilotomab monotherapy or combination with rituximab. Full circles: mice euthanized due to tumor diameter=20mm. Open circles: mice euthanized due to tumor-ulceration. Diamonds: mice euthanized due to end of study (at 114 days) or due to symptoms of sickness or discomfort.

TABLES

Table 1 Fold-change in average tumor volume from baseline of combination therapies vs corresponding monotherapies and Bliss synergy interaction values with 90% confidence intervals.

Study day	^{177}Lu-lilotomab (MBq/kg)	Fold-change from day 0		Interaction value (90% CI)
		-rituximab	+rituximab	
3	0	2.2	2.2	
	150	1.7	1.6	0.99 (0.41, 2.37)
	350	2.3	1.7	0.77 (0.32, 1.84)
7	0	6.1	5.5	
	150	3.3	2.4	0.80 (0.33, 1.91)
	350	2.7	1.6	0.66 (0.28, 1.57)
9	0	9.2	8.9	
	150	4.4	3.0	0.70 (0.29, 1.68)
	350	3.1	1.6†	0.53 (0.22, 1.23)
10	0	11.8	10.6	
	150	4.3	3.1	0.79 (0.33, 1.89)
	350	3.2	1.7	0.61 (0.26, 1.46)
13	0	20.4	16.6	
	150	5.0	3.2	0.79 (0.33, 1.89)
	350	3.1	1.3†	0.51 (0.22, 1.23)
15	0	36.2	28.8	
	150	5.7	3.3	0.74 (0.31, 1.77)
	350	3.3	1.3†	0.50 (0.21, 1.21)
17	0	57.8	42.6	
	150	7.7	3.5*	0.61 (0.25, 1.47)
	350	3.5	1.0†	0.39 (0.16, 0.94)‡
20	0	116.6	80.2	
	150	10.2	4.2*	0.60 (0.25, 1.43)
	350	4.1	1.0†	0.36 (0.15, 0.86)‡

*significant rituximab effect with 150MBq/ kg ^{177}Lu-lilotomab ($p<0.05$)

†significant rituximab effect with 350MBq/ kg ^{177}Lu-lilotomab ($p<0.05$)

‡significant synergism ($p<0.05$)

Table 2 Median survival time of mice treated with NaCl, rituximab, 150 and 350MBq/kg ^{177}Lu-lilotomab and combination therapies with 20mm tumor diameter as endpoint.

Treatment Group	Median survival±SE (days)
4×NaCl	13±0
4×10mg/kg rituximab	13±3
150MBq/kg ^{177}Lu-lilotomab	24±4*,†
350MBq/kg ^{177}Lu-lilotomab	38±11*,†
150MBq/kg ^{177}Lu-lilotomab+rituximab	31±5*,†
350MBq/kg ^{177}Lu-lilotomab+rituximab	70±8*,†
*Significantly different from NaCl ($p<0.001$)	
†Significantly different from 4x10mg/kg rituximab ($p<0.01$)	

Table 3 Bliss synergy interaction values calculated using the hazards found through Cox Proportional-Hazards model fitting to the mice survival (end point: tumor diameter larger than 20mm).

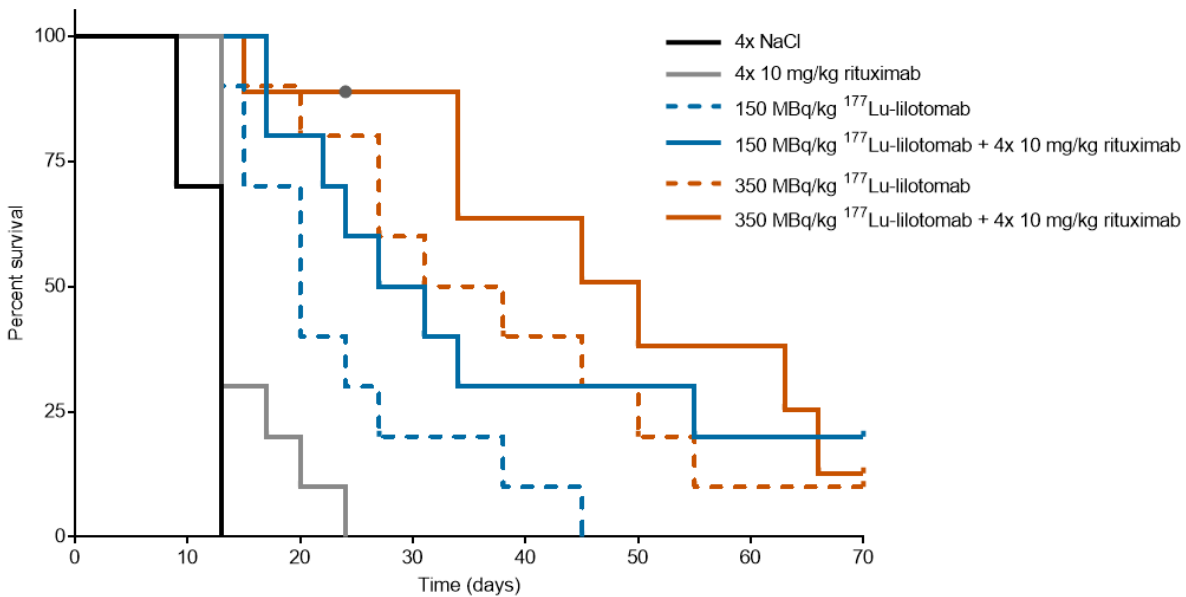|	Interaction Value (90% confidence interval)	p-value
150MBq/kg ^{177}Lu-lilotomab+rituximab	0.88 (0.30-2.63)	0.85
350MBq/kg ^{177}Lu-lilotomab+rituximab	0.83 (0.22-3.15)	0.82

Supplementary Data

Bliss independence analysis of tumor volume

Bliss analysis of tumor volume was performed using extrapolation of tumor volumes and was restricted to the first 20 days of the study. This was because there were no control animals beyond study day 13 and any analysis beyond day 20 would impose uncertainty. The tumor volumes were log transformed and data for mice withdrawn before study day 20 were extrapolated by linear regression. Beyond day 20 tumor sizes become infeasibly large. Difference from baseline was calculated on the log scale and all statistical analysis were performed on the log-transformed data. A mixed effects linear model was used including fixed effects of each of the treatments (referred to as between group factors) and the associated interaction between these factors. Additionally, study day was included as a within animal fixed effect. All the interactions between the group factors and study day were included. Animal within group and the side of the tumor were included as random effects in the model. An autoregressive correlation structure was assumed. The effects of treatment with and without rituximab were evaluated separately at each dose of ^{177}Lu-lilotomab (control, 150 MBq/kg and 350 MBq/kg), for each study day. The size of these effects was compared for 150 MBq/kg ^{177}Lu-lilotomab against the control and 350 MBq/kg ^{177}Lu-lilotomab against the control using the interaction test of the Bliss independence model using SAS 9.4 (SAS Institute, NC, USA). Interaction values less than 1 were considered synergistic and statistical significance defined by $p < 0.05$.

Survival and Bliss synergy analysis with endpoint criteria: >20 mm tumor diameter and tumor-ulceration

Treatment with ^{177}Lu-lilotomab alone and in combination with rituximab significantly prolonged survival compared to saline and rituximab treatment (Supplemental Fig.1, Supplemental Table 1). However, treatment with ^{177}Lu-lilotomab in combination with rituximab did not significantly differ from treatment with rituximab alone.

Bliss independence analysis did not provide statistically significant results (Supplemental Table 2). However, with only 10 mice per group the hazard proportionality is an approximation. The lack of significance is because of the poor Proportional Hazards assumption in the Cox model (p = 0.07).

Supplemental Fig.1 Kaplan-Meier survival curves of Raji2R-xenografted mice treated with saline, rituximab, 150 MBq/kg and 350 MBq/kg ^{177}Lu-lilotomab monotherapy or combination with rituximab. N=10. Gray dots: censored animals.

Supplemental Table 1 Median survival time of mice treated with NaCl, rituximab, 150 and 350MBq/kg ^{177}Lu-lilotomab and combination therapies.

Treatment Group	Median survival ± SE (days)
4×NaCl	13±0
4×10mg/kg rituximab	13±3
150MBq/kg ^{177}Lu-lilotomab	20±3*,†
350MBq/kg ^{177}Lu-lilotomab	38±9*,†
150MBq/kg ^{177}Lu-lilotomab + rituximab	27±6*,†
350MBq/kg ^{177}Lu-lilotomab + rituximab	50±7*,†
*Significantly different from NaCl ($p<0.001$)	
†Significantly different from 4x10 mg/kg rituximab ($p<0.01$)	

Supplemental Table 2 Bliss synergy interaction values

	Interaction Value* (90% confidence interval)	p-value
150 MBq/kg ^{177}Lu-lilotomab + rituximab	0.7 (0.43-1.25)	0.54
350 MBq/kg ^{177}Lu-lilotomab + rituximab	1.58 (0.61-4.08)	0.43

*calculated using the hazards found through Cox Proportional Hazards model fitting to mouse survival.
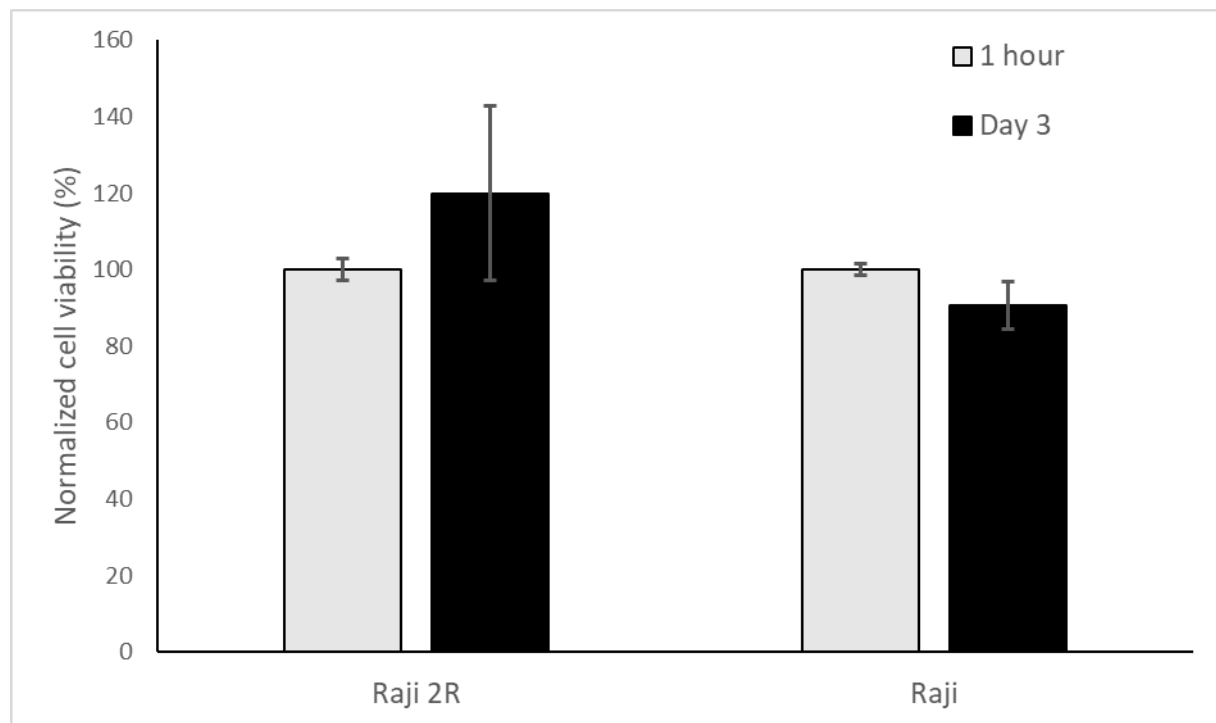
Measurement of cell viability and apoptosis (Method)

At a concentration of 2.5×10^5 cells/ml, Raji and Raji2R cells were incubated at 37°C with either 50μg/ml rituximab or PBS. At 1 hour and 3 days after start of incubation, the cells were transferred to 96 well plates and incubated with RealTime-Glo™ MT Cell Viability Assay (Promega, USA) following the manufacturer's protocol. The luminescence, proportional to the number of viable cells, was measured at each timepoint on a Spark microplate reader (TECAN, Switzerland). The experiment was performed in duplicates and the results are presented as mean± standard deviation (SD).
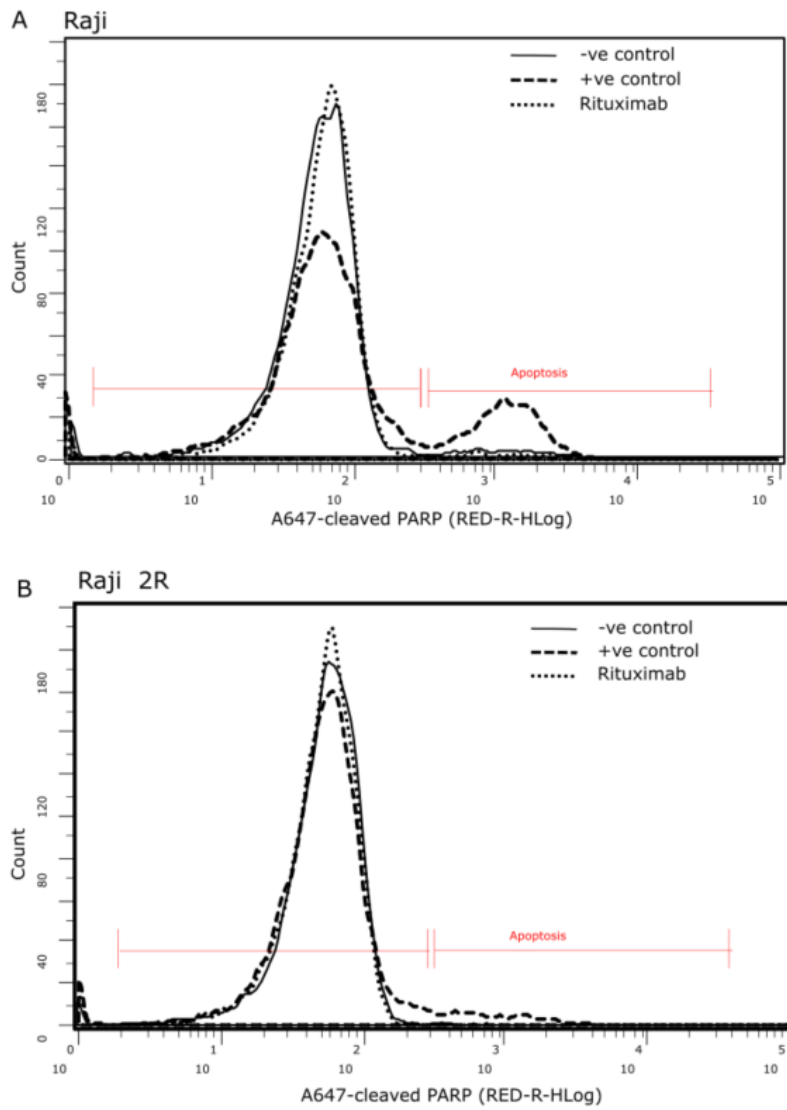
On day 3, 2.0×10^6 cells were fixed using ice cold methanol in preparation for evaluation of apoptosis by flow cytometry analysis. A positive control was included in the study by incubating the unfixed control cells with a topoisomerase inhibitor; etoposide, for 18 hours prior to analysis. The fixed cells were then washed and incubated with Alexa conjugated anti-cleaved PARP antibody (BioNordika, Norway) diluted 1:100 in 5% non-fat milk for 1 hour. The cells were once again washed, and the fluorescent apoptosis signal determined by flow cytometry (Guava® easyCyte12HT, Millipore).

Effect of rituximab treatment on cell viability and apoptosis (Results)

Treatment with rituximab did not yield any significant effect on cell viability relative to the untreated cells after 1 hour and on day 3 for both Raji and Raji2R cells (Supplemental Fig. 2). In addition, treatment of Raji and Raji2R cells with rituximab had no significant effect on initiating apoptosis. The percentage of total number of apoptotic cells in rituximab treated Raji cells was similar to those in the untreated control cells at day 3 (Supplemental Fig.3). Raji 2R cells were overall resistant to rituximab treatment and no apoptosis was observed (Supplemental Fig. 3).

Supplemental Fig. 2 Effect of rituximab-treatment on viability in Raji and Raji2R cells. Mean ±SD, N=2

Supplemental Fig.3 Example histograms showing the change in induction of apoptosis after treatment of Raji and Raji 2R cells with PBS as a negative control, etoposide as a positive control denoted as -ve and +ve control respectively or 50µg/ml rituximab.